CHEMISTRY
A EUROPEAN JOURNAL

ChemPubSoc
Europe

DOI: 10.1002/chem.201103385

A Nucleobase-Discriminating Pyrrolo-dC Click Adduct Designed for DNA Fluorescence Mismatch Sensing

Xin Ming[a] and Frank Seela*[a, b]

Abstract: New pyrrolo-dC click adducts (**4** and **5**) tethered with a 1,2,3-triazole skeleton were synthesized and oligonucleotides were prepared. The triazole system was either directly linked to the pyrrolo moiety (**5**) or connected via an *n*-butyl linker (**4**). The quantum yield of nucleoside **5** ($\Phi =$ 0.32), which is 10 times higher than those of 8-methylpyrrolo-dC (**1b**, $\Phi =$ 0.026) or the long linker derivative **4** ($\Phi = 0.03$), is maintained in oligonucleotides. Compound **5** was used as a nucleobase-discriminating fluorescence sensor in duplex DNA. Excellent mismatch discrimination was observed when **5** was positioned opposite the four canonical nucleosides. Compound **5** has the potential to be used for SNP detection in long DNA targets when conventional techniques such as high resolution melt analysis fail.

Keywords: click chemistry · deazapurines · fluorescence · oligonucleotides · sensors

Introduction

Fluorescence is widely used to explore the structure, dynamics, and interactions of nucleic acids.[1] As canonical bases of nucleic acids are almost nonemissive, numerous fluorescent nucleoside analogues including those that participate in charge transfer[2] have been synthesized and incorporated into DNA.[3] An attractive feature of emissive nucleobase analogues[4] that closely resemble natural nucleosides is that they do not perturb DNA structure and retain nucleobase recognition.[5] A valuable addition to the realm of fluorescent pyrimidine nucleoside analogues available for probing nucleic acid interactions is pyrrolo-dC (**1a**)[6] and pyrrolo-C.[7] These molecules with intrinsic fluorescence represent pyrrolo[2,3-*d*]pyrimidin-2-one derivatives in which nitrogen-1 acts as a glycosylation site.[8] 7-Deaza-2′-deoxyisoinosine, a related nucleoside with a regular glycosylation site (*N*-9) is also fluorescent and has been incorporated in oligonucleotides (purine numbering is used throughout the results and discussion section).[9] The 8-methyl derivative of pyrrolo-dC (^{me}pyrrolo-dC, **1b**)[10] has been successfully used for the characterization of elongation complexes of T7 RNA polymerase,[11] as a biosensor for metal-ion detection,[12] and to determine local structure changes in double-stranded DNA[13] or in DNA/RNA hybrids.[14] Fluorescent ^{me}pyrrolo-dC (**1b**) forms stable tridentated base pairs with dG, similar to dC.[11a]

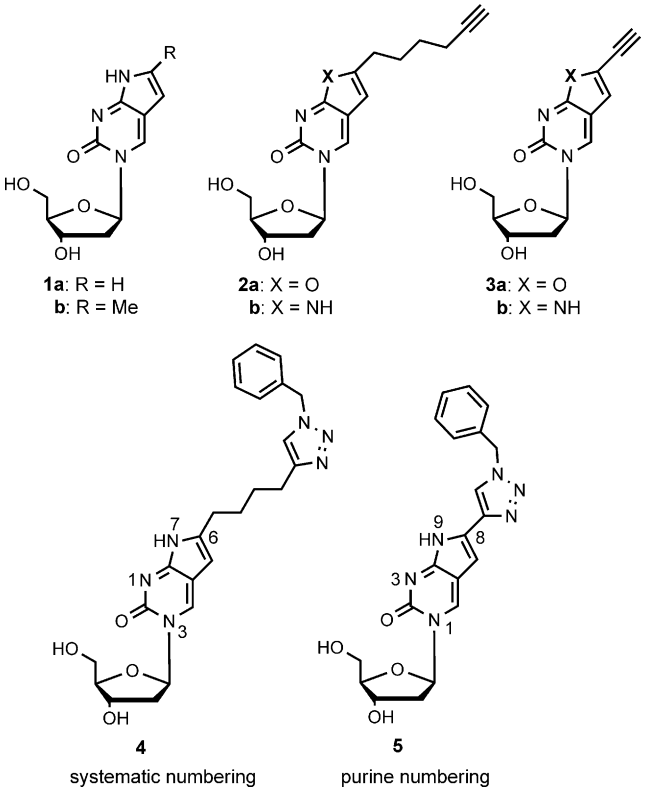

Recently, our laboratory has reported on the pyrrolo-dC derivative **2b** and its furano[2,3-*d*]pyrimidine precursor **2a** decorated with an 8-hexynyl side chain. The influence on base-pair stability and mismatch discrimination was investi-

[a] Dr. X. Ming, Prof. Dr. F. Seela
Laboratory of Bioorganic Chemistry and Chemical Biology
Center for Nanotechnology
Heisenbergstraße 11, 48149 Münster (Germany)
Fax: (+49) 251-53406857
E-mail: frank.seela@uni-osnabrueck.de

[b] Prof. Dr. F. Seela
Laboratorium für Organische und Bioorganische Chemie
Institut für Chemie, Universität Osnabrück
Barbarastraße 7, 49069 Osnabrück (Germany)
Fax: (+49) 251-53406857
E-mail: frank.seela@uni-osnabrueck.de

Supporting information for this article is available on the WWW under http://dx.doi.org/10.1002/chem.201103385.

gated.[15] Nucleoside **2b** was further functionalized by the copper(I)-catalyzed Huisgen–Meldal–Sharpless 1,3-dipolar cycloaddition ('click' chemistry)[16] with fluorogenic azidocoumarin.[15] Relative to other fluorescent nucleosides, such as 2-aminopurine 2′-deoxyribonucleoside, ^{me}pyrrolo-dC (**1b**) develops only a moderate fluorescence with a quantum yield Φ of 0.026.[17] Earlier, it was shown that a 1,2,3-triazole moiety introduced at the 8-position of 2′-deoxyadenosine induced fluorescence.[18] Consequently, we reasoned that the incorporation of a 1,2,3-triazole moiety at the 8-position of the pyrrolo-C nucleobase might enhance fluorescence quantum yield. The expected favorable photophysical properties would be useful for fluorescence sensing. As nucleobase discriminatory sensing can be performed on duplex DNA at a defined temperature it shows advantages over methods using high-resolution melt analysis (HRM), which is limited to short DNA fragments, whereas fluorescence sensing can be applied to long DNA duplexes.

This manuscript reports on pyrrolo-dC benzyl azide click adducts in which the triazole moiety is directly attached to the pyrrolo[2,3-*d*]pyrimidine skeleton (**5**) or is connected via an *n*-butyl spacer (**4**). Click conjugates **4** and **5** and phosphoramidites and oligonucleotides containing these modified nucleosides were prepared. The impact of the triazole moiety on fluorescence, base-pairing, and mismatch discrimination was evaluated to develop a highly emissive new nucleoside mimic to detect single-nucleotide polymorphism (SNP) by fluorescence sensing.[19]

Results and Discussion

Synthesis of monomers: In compliance with standard protocols, pyrrolo-dC derivatives are obtained from corresponding furano-dU precursors, which are accessible from 5-alkynylated dU nucleosides by cyclization with copper iodide.[10,20] For oxygen→nitrogen exchange, the respective furano[2,3-*d*]pyrimidine nucleosides are treated with ammonia. Accordingly, compound **3a** was prepared by following a literature protocol.[21] Then, the copper(I)-catalyzed 'click' reaction was performed on **3a** with benzyl azide (**6**) to afford **7** in 70% yield. Unexpectedly, treatment of **7** with concentrated aqueous ammonia did not result in oxygen–nitrogen exchange; instead of **5**, an inseparable mixture of reaction products was formed (Scheme 1).

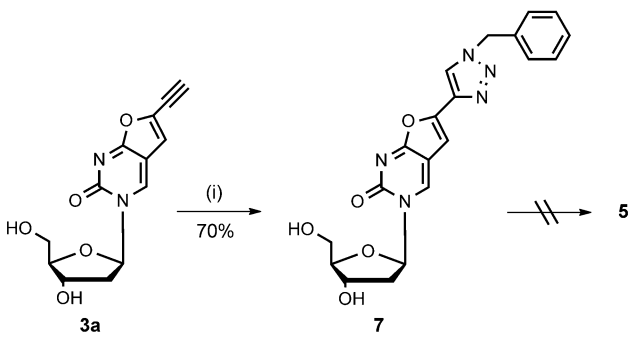

Scheme 1. Predicted route for the synthesis of nucleoside **5**. i) $CuSO_4$, sodium ascorbate, *t*BuOH/H_2O, benzyl azide **6**.

Thus, we changed our synthetic strategy and made use of the Sonogashira cross-coupling reaction to connect the side chain with the pyrrolo-dC system (Scheme 2). Such a protocol was already reported for the synthesis of related nucleosides.[22] 1-Benzyl-4-ethynyl-1*H*-1,2,3-triazole (**9**) was synthesized as a side-chain precursor. For this, the click reaction was performed on 1,4-(bis-trifluoromethyl)silyl-buta-1,3-diyne (**8**) with benzyl azide (**6**) in the presence of CuBr/DMF.[23] Then, the one-pot Sonogashira cross-coupling of alkyne **9** with N^4-benzoyl-5-iodo-5′-dimethoxytrityl-2′-deoxycytidine (**10**) by using CuI, $[PdCl_2(PPh_3)_2]$/Et_3N was performed yielding **11** (50% yield).[6,22] The DMT-residue was removed with 2.5% dichloroacetic acid to give nucleoside **5** (87%). Treatment of **11** with 2-cyanoethyl-*N*,*N*-diisopropylphosphoramido chloridite afforded the phosphoramidite **12** (75% yield; Scheme 2).

Next, the pyrrolo-dC nucleoside **4** with the *n*-butyl linker was synthesized (Scheme 3). The reported 8-hexynyl-pyrrolo-dC (**2b**)[15] was used as the starting material. Compound **2b** was clicked with benzyl azide **6** to afford compound **4**

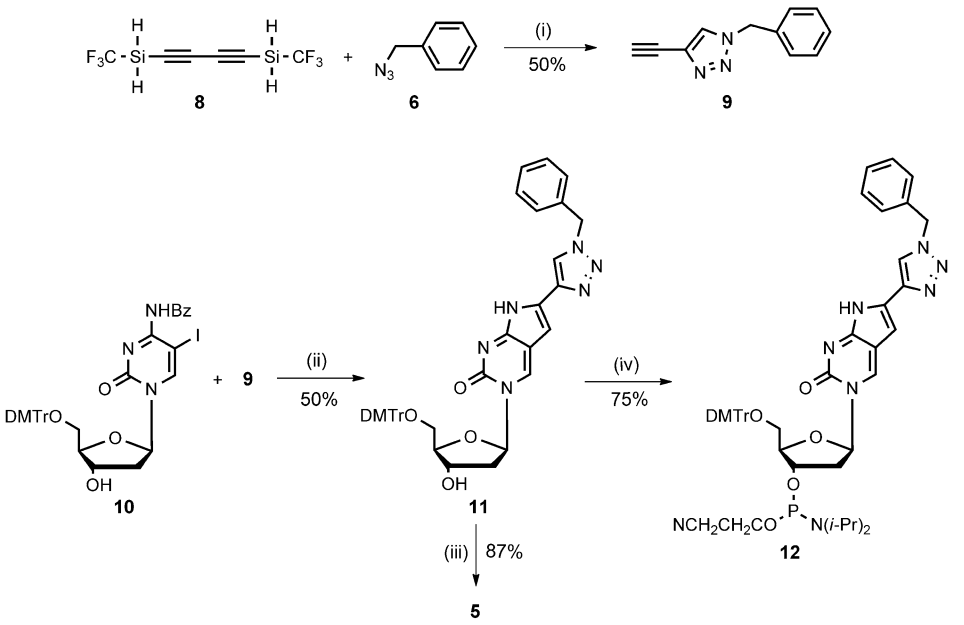

Scheme 2. Synthetic route for the preparation of nucleoside **5** and phosphoramidite **12**. i) CuBr, Et_3N, H_2O, DMF, 100°C; ii) CuI, $[PdCl_2(PPh_3)_2]$, Et_3N, 50°C; iii) 2.5% dichloroacetic acid; iv) $NC(CH_2)_2OP(Cl)N(iPr)_2$.

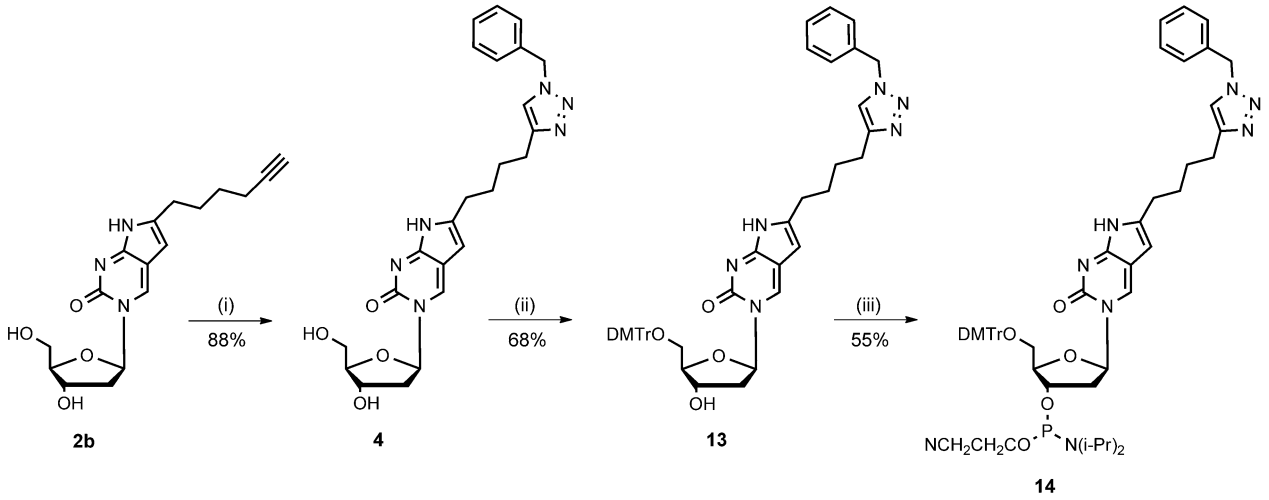

Scheme 3. Synthesis of nucleoside **4** and phosphoramidite **14**. i) $CuSO_4$, sodium ascorbate, *t*BuOH/H_2O, benzylazide (**6**); ii) DMTr-Cl, pyridine; iii) NC-$(CH_2)_2OP(Cl)N(iPr)_2$.

(88% yield). The latter was converted to the DMT derivative **13** (68%) and phosphitylation gave phosphoramidite **14** (55%).

All compounds were characterized by ^1H, ^{13}C, and ^{31}P NMR spectra and by elemental analyses. The ^{13}C NMR signals were assigned from ^1H–^{13}C gated-decoupled spectra (Supporting Information). The ^{13}C NMR chemical shifts are compiled in Table 4 (Experimental Section).

Photophysical properties of pyrrolo-dC adducts: ^{me}Pyrrolo-dC (**1b**) shows fluorescence, but has a rather low quantum yield ($\Phi = 0.026$).[17] Compound **4**, in which the triazole moiety is tethered to the pyrrolo system via an *n*-butyl spacer, shows a similar quantum yield ($\Phi = 0.03$). Interestingly, the quantum yield of adduct **5** containing the 1,2,3-triazole system in direct conjugation to the pyrrolo-dC moiety is about 10 times higher ($\Phi = 0.32$), and this compound shows blue emission. The quantum yield of the related 8-phenyl pyrrolo-dC is within the same range ($\Phi = 0.31$).[24] In addition, the parent furano[2,3-*d*]pyrimidine precursor **7** shows a similar quantum yield ($\Phi = 0.30$) (Table 1). Apparently, conjugation of an aromatic system with the pyrrolo-dC base has a positive effect on the fluorescence properties.

Table 1. Photophysical properties of fluorescent nucleosides.[a]

Compound	λ_{max} [nm]	ε_{max} [$mol^{-1}dm^3cm^{-1}$]	Ex_{max} [nm]	Em_{max} [nm]	Quantum yield (Φ)[b]	Brightness[e]
^{me}pyrrolo-dC	340	3500	341	457	0.03	105
(**1b**)	(340)[c]	(3500)[c]	(350)[c]	(460)[c]	(0.026)[c]	(91)[c]
pyrrolo-C[7a]	344[d]	3100[d]	336	450	0.06	186
2b[15]			340	466	0.05	
4	340	3600	341	456	0.03	108
5	354	8500	355	450	0.32	2720
3a			336	416	0.08	
7			339	422	0.30	

[a] UV and fluorescence spectra were measured in water containing 0.5% DMSO. [b] Quantum yields were determined by using quinine sulphate in 0.1 N H_2SO_4 as a standard with $\Phi = 0.54$. [c] Data in parentheses were taken from reference [17]. [d] Determined in methanol. [e] The brightness was calculated as: brightness $= \varepsilon_{max}\Phi$.

The excitation and emission maxima of compounds **4** and **5** are not in the range of the absorption bands of DNA (Table 1 and Figure 1). Consequently, the DNA nucleobases do not interfere with the excitation wavelengths. Both compounds show Stoke's shifts of around 100 nm.

As we considered to use compounds **4** and **5** for fluorescence sensing, it was important that fluorescence changes induced by the partner base within a base pair are not superimposed by pH-dependent fluorescence changes (pK_a out of the range of fluorescence sensing) of the sensor molecules (**4** or **5**). To exclude these problems, titration experiments monitoring fluorescence changes were performed (Figure 2). Corresponding UV measurements are shown in the Supporting Information (see Figures S9 and S10). The pK_a values of protonation are 2.6 (for **4**, Figure 2a) and 2.7 (for **5**, Figure 2b), which are about 2 units lower than that of dC ($pK_a = 4.3$).[25] The protonation sites were tentatively assigned to *N*-3. Titration under alkaline conditions afforded a second pK_a value for both nucleosides (12.0 for **4** and 10.9 for **5**, Figure 2). In this case, deprotonation of the pyrrole nitrogen (*N*-9) is anticipated. Taken together, fluorescence sensing at physiological conditions (between pH 4 and 10) is not disturbed by fluorescence changes of the sensor molecules **4** or **5**.

Oligonucleotide synthesis, base-pair stability, and mismatch discrimination: Solid-phase oligonucleotide syntheses were performed by employing the phosphoramidites **12** or **14** and standard building blocks. For details, see the Supporting Information. To investigate the influence of nucleosides **4** or **5** on the stability of non-self-complementary duplexes, a series of oligonucleotides was synthesized containing either **4** or **5**. For that, the duplexes 5′-d(TAGGTCAATACT) (**15**) and 3′-d(ATCCAGT-

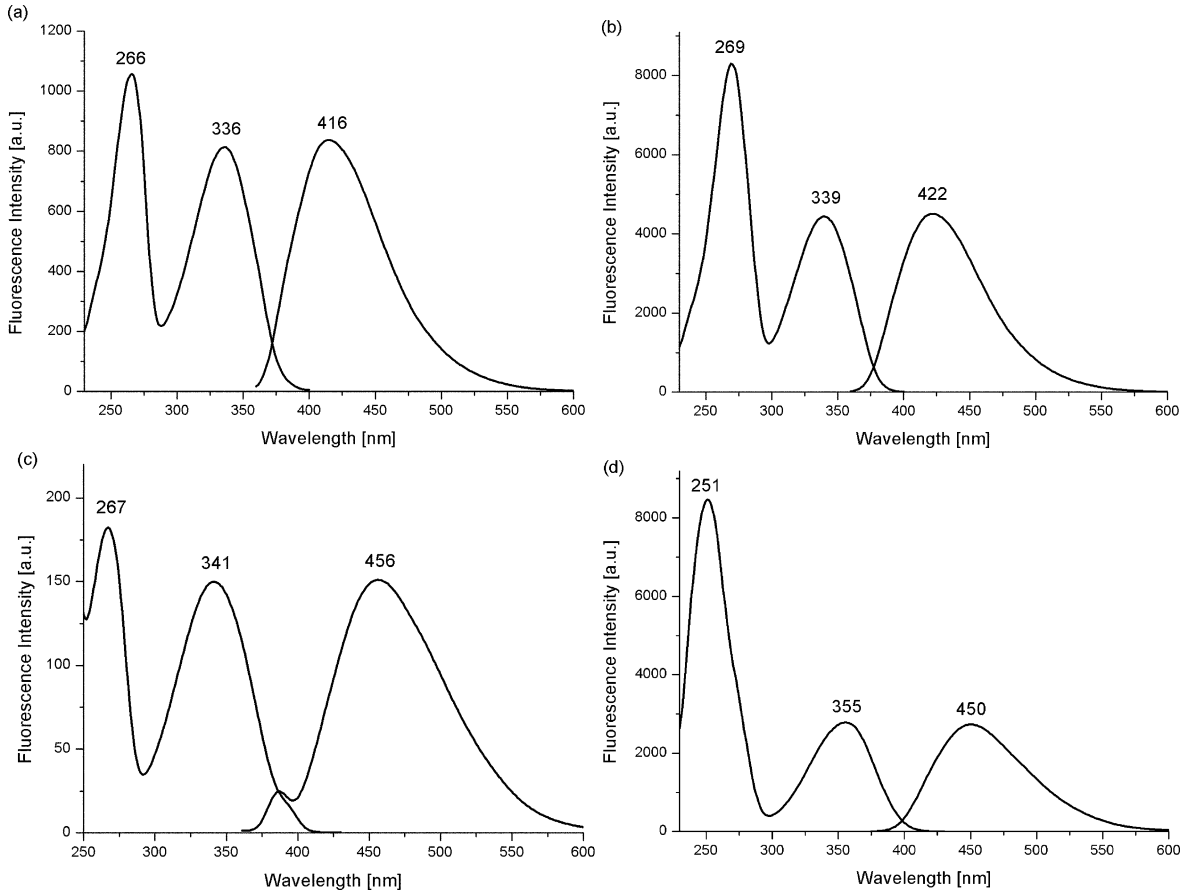

Figure 1. Fluorescence excitation and emission spectra of compound **3a** (a), **7** (b), **4** (c), and **5** (d) measured in water containing 0.5% DMSO at a concentration of 2.5 μM each.

TATGA) (**16**) were used as a reference. At different positions, dC residues were replaced by nucleoside **4** or **5** resulting in oligonucleotides **17–24** (Table 2).

The data of Table 2 show that modifications at the center of the duplexes have a stronger impact on T_m changes than modifications at the end of the duplex. Stability depends also on the connectivity of the pyrrole ring to the triazole tether. A positive influence on duplex stability occurs when the triazole moiety is directly attached to the nucleobase as in compound **5**, whereas a triazole residue separated from the nucleobase by an *n*-butyl spacer (**4**) led often to a decrease in T_m values. The most stable duplexes were formed when a central dC was replaced by compound **5** (**17·16**). T_m values determined at high salt (1 M NaCl) are usually 3–6 °C higher than those measured at low salt conditions (0.1 M NaCl). Base-pair motifs **I** and **II** can be anticipated for all oligonucleotide duplexes.

It has been shown that ^{me}pyrrolo-dC (**1b**) hybridizes strongly with dG and discriminates the other canonical nucleosides.[3,10] From this background and the high quantum yield of **5**, the base discriminating properties of oligonucleotides incorporating nucleoside **4** or **5** against canonical nucleosides were investigated (Table 3). For this study, a set of single-stranded oligonucleotides (**16**, **25–27**) was hybridized with the complementary strand **17**, **18**, or **21** resulting in the duplexes shown in Table 3. Melting experiments were per-

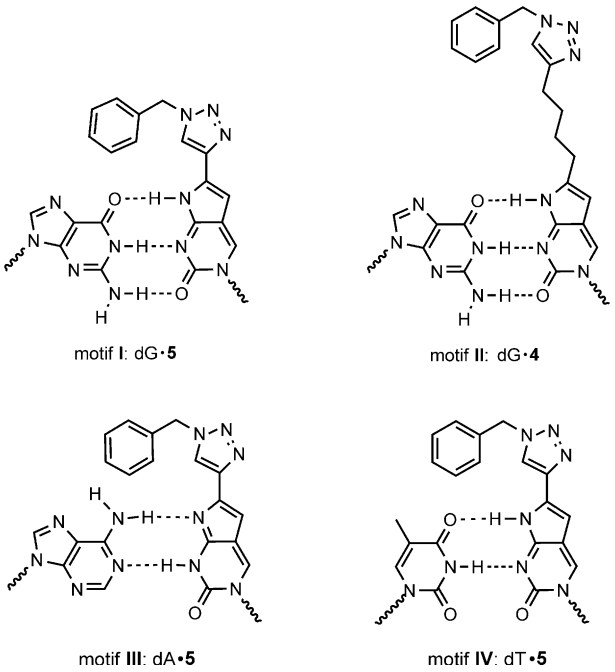

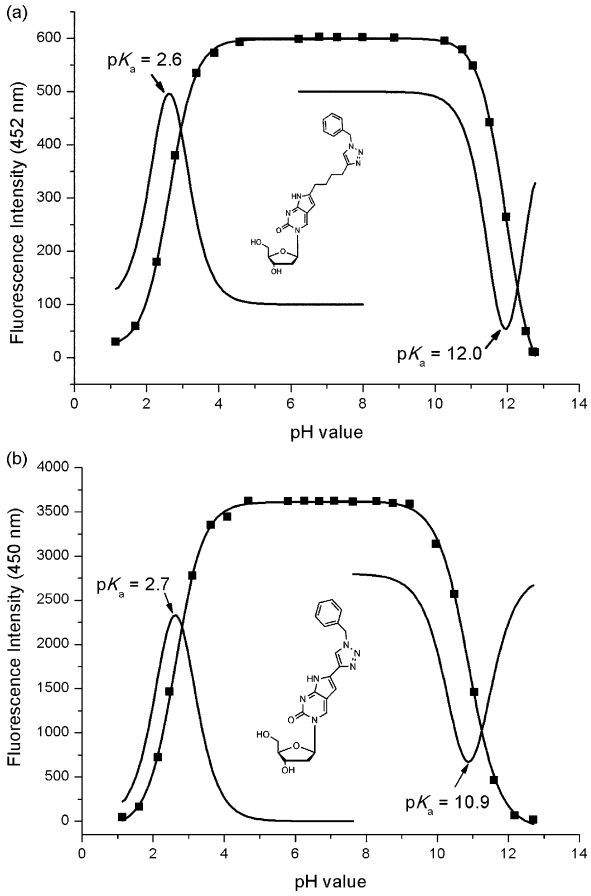

Figure 2. a) Graph of fluorescence emission at 452 nm against pH value and its first derivative using data from pH-dependent fluorescence spectra of nucleoside **4** measured in 0.1 M sodium phosphate buffer (excitation wavelength: 342 nm). b) Graph of fluorescence emission at 450 nm against pH value and its first derivative using data from pH-dependent fluorescence spectra of nucleoside **5** measured in 0.1 M sodium phosphate buffer (excitation wavelength: 356 nm).

formed at high (1 M NaCl) and low salt (0.1 M NaCl, data in parentheses) conditions. At high salt concentration, the mispairs of **4**-dC (**21·25**, $\Delta T_m = -25\,^{\circ}C$) and **5**-dC (**17·25**, $\Delta T_m = -24\,^{\circ}C$) showed the largest T_m decrease, comparable to the corresponding dC–dC mispair (**15·25**, $\Delta T_m = -24\,^{\circ}C$). On the contrary, the fully matched duplexes **21·16** and **17·16** containing **4**-dG or **5**-dG base pairs show the highest T_m values. The T_m value of 43 °C for duplex **17·26** containing a **5**-dA pair is in the range of duplex **17·27** bearing a **5**-dT pair. Such base pairs are possible when the pyrrolo-C nucleobase forms other tautomers as shown by motif **III** and motif **IV**. Corresponding measurements at low salt conditions generally resulted in 2–6 °C lower T_m values. It is further observed that mismatches of **5** with canonical nucleosides are more stable than corresponding dC mismatches, and nucleosides **4** and **5** differ slightly in mismatch discrimination. We anticipate that this results from the direct conjugation of the triazole system.

Fluorescence sensing experiments with nucleosides 4 and 5: Nucleobase-discriminating nucleosides with intrinsic fluorescence have been studied by the groups of Saito, Hudson, and others.[20b,26] Our laboratory has reported on nucleobase discrimination by fluorescence sensing of canonical nucleosides by utilizing 8-aza-2′-deoxyguanosine and 8-aza-2′-deoxyisoguanosine that are strongly fluorescent as anions.[27] Fluorescence sensing experiments are primarily designed for single-nucleotide polymorphism (SNP) analysis and are performed at a defined temperature to give "snap shots" of an emissive nucleoside within a particular DNA environment. Commonly, fluorescent nucleoside probes are placed opposite to nucleobases of interest to detect different fluorescence signals. Ideally, the obtained steady-state fluorescence changes can be correlated to particular matches or mismatches due to microenvironmental changes. Different to nucleobase discrimination by fluorescence sensing, duplex melting experiments monitor UV changes within a cooperative melting process occurring within a certain temperature range. Thus, both methods monitor different events that might not lead to identical results. Nevertheless, our laboratory and others showed that data obtained for mismatch discrimination by fluorescence sensing often match the results received by T_m measurements.[20b,26a,27a]

At first experiments were performed by using temperature-dependent fluorescence intensity changes for T_m determination. For this, the same oligonucleotide duplexes with nucleoside **5** were used for UV melting (Table 3). We had to consider that fluorescence decreases with increasing temperature and that this effect superimposes the fluorescence increase caused by duplex melting. As a result, only modest temperature-dependent melting profiles were observed in some cases. The situation was even more complex for duplex **17·26** (dA-**5**) as the fluorescence intensity of the double strand was rather close to that of the single-stranded oligonucleotide **17**. Thus, we measured the fluorescence decrease of the single strand **17** containing the sensor separately and used these data for the correction of fluorescence curves (Supporting Information). When the quotient of the fluorescence intensity of the original melting curves and the single strand fluorescence decrease was formed, perfect sigmoidal melting profiles were obtained (for details see Figures S13–S16 in the Supporting Information).[28] The results are summarized in Figure 3b and are correlated to the data obtained by UV melting (Figure 3a). Both methods reflect the same order of duplex stabilities, although minor T_m differences are occurring.

The experiments discussed above indicate that fluorescence melting used for mismatch discrimination shows disadvantages already for short DNA duplexes. This is a result of the relative low fluorescence of nucleobase analogues relative to fluorescent dye tags. Nevertheless, fluorescent nucleoside analogues such as compound **5** monitor matches and mismatches directly as they are part of the base-pair motifs. Dye tags communicate conformational changes in a more indirect way.

Table 2. T_m values of oligonucleotide duplexes containing the modified pyrrolo-dC nucleosides **4** and **5**.[a]

Duplex	T_m [°C]	ΔT_m[b] [°C]	Duplex	T_m [°C]	ΔT_m[b] [°C]
5′-d(TAG GTC AAT ACT) (**15**)	51	–			
3′-d(ATC CAG TTA TGA) (**16**)	(48)	–			
5′-d(TAG GT**5** AAT ACT) (**17**)	55	+4	5′-d(TAG GT**4** AAT ACT) (**21**)	51	0
3′-d(ATC CAG TTA TGA) (**16**)	(50)	(+2)	3′-d(ATC CAG TTA TGA) (**16**)	(46)	(−2)
5′-d(TAG GTC AAT A**5**T) (**18**)	51	0	5′-d(TAG GTC AAT A**4**T) (**22**)	50	−1
3′-d(ATC CAG TTA TGA) (**16**)	(48)	(0)	3′-d(ATC CAG TTA TGA) (**16**)	(46)	(−2)
5′-d(TAG GT**5** AAT A**5**T) (**19**)	53	+2	5′-d(TAG GT**4** AAT A**4**T) (**23**)	47	−4
3′-d(ATC CAG TTA TGA) (**16**)	(48)	(0)	3′-d(ATC CAG TTA TGA) (**16**)	(43)	(−5)
5′-d(TAG GTC AAT ACT) (**15**)	52	+1	5′-d(TAG GTC AAT ACT) (**15**)	48	−3
3′-d(AT**5 5**AG TTA TGA) (**20**)	(48)	(0)	3′-d(AT**4 4**AG TTA TGA) (**24**)	(45)	(−3)
5′-d(TAG GT**5** AAT ACT) (**17**)	57	+6	5′-d(TAG GT**4** AAT ACT) (**21**)	47	−4
3′-d(AT**5 5**AG TTA TGA) (**20**)	(52)	(+4)	3′-d(AT**4 4**AG TTA TGA) (**24**)	(43)	(−5)
5′-d(TAG GTC AAT A**5**T) (**18**)	49	−2	5′-d(TAG GTC AAT A**4**T) (**22**)	45	−6
3′-d(AT**5 5**AG TTA TGA) (**20**)	(45)	(−3)	3′-d(AT**4 4**AG TTA TGA) (**24**)	(43)	(−5)
5′-d(TAG GT**5** AAT A**5**T) (**19**)	54	+3	5′-d(TAG GT**4** AAT A**4**T) (**23**)	43	−8
3′-d(AT**5 5**AG TTA TGA) (**20**)	(48)	(0)	3′-d(AT**4 4**AG TTA TGA) (**24**)	(40)	(−8)

[a] Measured at 260 nm in a 1 M NaCl solution containing 100 mM $MgCl_2$ and 60 mM Na-cacodylate (pH 7.0) with 5+5 μM single-strand concentration. Data in parentheses refer to measurements in 0.1 M NaCl, 10 mM $MgCl_2$, 10 mM Na-cacodylate, pH 7.0. [b] ΔT_m was calculated as $T_m^{\text{modified duplex}} - T_m^{\text{unmodified duplex}}$ by using **15·16** as a comparison.

Table 3. T_m values of oligonucleotide duplexes containing the pyrrolo-dC nucleosides **4** and **5** located opposite canonical nucleosides.[a]

Duplex	T_m [°C]	ΔT_m[b] [°C]	Duplex	T_m [°C]	ΔT_m[b] [°C]
5′-d(TAG GT**5** AAT ACT) (**17**)	55	–	5′-d(TAG GT **4** AAT ACT) (**21**)	51	–
3′-d(ATC CA**G** TTA TGA) (**16**)	(50)	–	3′-d(ATC CA**G** TTA TGA) (**16**)	(46)	–
5′-d(TAG GT**5** AAT ACT) (**17**)	31	−24	5′-d(TAG GT **4** AAT ACT) (**21**)	26	−25
3′-d(ATC CA**C** TTA TGA) (**25**)	(27)	(−23)	3′-d(ATC CA**C** TTA TGA) (**25**)	(24)	(−22)
5′-d(TAG GT**5** AAT ACT) (**17**)	43	−12	5′-d(TAG GT**4** AAT ACT) (**21**)	29	−22
3′-d(ATC CA**A** TTA TGA) (**26**)	(38)	(−12)	3′-d(ATC CA**A**TTA TGA) (**26**)	(27)	(−19)
5′-d(TAG GT**5** AAT ACT) (**17**)	42	−13	5′-d(TAG GT **4** AAT ACT) (**21**)	35	−16
3′-d(ATC CA**T** TTA TGA) (**27**)	(36)	(−14)	3′-d(ATC CA**T** TTA TGA) (**27**)	(29)	(−18)
5′-d(TAG GT**C** AAT A**5**T) (**18**)	51	–	5′-d(TAG GT**C** AAT ACT) (**15**)	51	–
3′-d(ATC CA**G** TTA TGA) (**16**)	(48)	–	3′-d(ATC CA**G** TTA TGA) (**16**)	(48)	–
5′-d(TAG GT**C** AAT A**5**T) (**18**)	22	−29	5′-d(TAG GT**C** AAT ACT) (**15**)	27	−24
3′-d(ATC CA**C** TTA TGA) (**25**)	(23)	(−25)	3′-d(ATC CA**C** TTA TGA) (**25**)	(23)	(−25)
5′-d(TAG GT**C** AAT A**5**T) (**18**)	22	−29	5′-d(TAG GT**C** AAT ACT) (**15**)	28	−23
3′-d(ATC CA**A** TTA TGA) (**26**)	(22)	(−26)	3′-d(ATC CA**A** TTA TGA) (**26**)	(25)	(−23)
5′-d(TAG GT**C** AAT A**5**T) (**18**)	27	−24	5′-d(TAG GT**C** AAT ACT) (**15**)	32	−19
3′-d(ATC CA**T** TTA TGA) (**27**)	(22)	(−26)	3′-d(ATC CA**T** TTA TGA) (**27**)	(27)	(−21)

[a] Measured at 260 nm in a 1 M NaCl solution containing 100 mM $MgCl_2$ and 60 mM Na-cacodylate (pH 7.0) with 3+3 μM single-strand concentration. Data in parentheses refer to measurements in 0.1 M NaCl, 10 mM $MgCl_2$, 10 mM Na-cacodylate, pH 7.0. [b] ΔT_m was calculated as $T_m^{\text{modified duplex}} - T_m^{\text{unmodified duplex}}$ by using **17·16**, **21·16**, **18·16**, or **15·16** as a comparison.

It has been reported that ^{me}pyrrolo-dC (**1b**) shows intrinsic fluorescence, however, with a rather low quantum yield of $\Phi = 0.026$, which is not significantly decreased when the nucleoside is an integral part of a dinucleotide.[17] The fluorescence of ^{me}pyrrolo-dC (**1b**) even increases when incorporated into single-stranded oligonucleotides and was shown to be rather independent from flanking neighbors.[17] This is different to other nucleosides showing intrinsic fluorescence, such as 2-aminopurine[29] or 2-amino-7-deazapurine 2′-deoxyribonucleosides,[30] which are strongly quenched when incorporated into oligonucleotides. It was suggested that ^{me}pyrrolo-dC (**1b**) develops only weak stacking interactions,

Table 4. ^{13}C NMR chemical shifts (δ) of pyrrolo[2,3-*d*]pyrimidine derivatives.[a]

Cpd	C[2][b] C[2][c]	C[6][b] C[4][c]	C[5][b] C[4a][c]	C[7][b] C[5][c]	C[8][b] C[6][c]	C[4][b] C[7a][c]	C1′	C2′	C3′	C4′	C5′	Triazole	Phenyl	CH_2
4	153.9	134.5	108.8	96.4	142.2	159.2	86.7	41.4	70.0	87.8	61.0	136.3 122.0	128.7 128.0 127.8	52.6 28.4 27.1 24.7
5	153.8	136.6	108.7	96.7	139.5	159.4	87.0	41.4	69.9	87.9	61.0	135.7 121.9	130.9 128.9 128.3 128.1	53.1
7	153.7	138.6	106.1	99.8	146.4	170.9	87.7	41.2	69.7	88.2	60.8	137.6 123.5	135.6 128.8 128.3 128.1	53.2
11	153.8	136.0	108.6	96.3	139.4	158.1	86.8	41.5	69.3	85.8	62.8	121.8 135.7[d]	130.9[d] 128.9[d] 128.3[d] 128.1[d]	53.1
13	153.8	134.0	108.7	95.9	142.2	159.2	86.4	41.5	69.3	85.6	62.8	136.3 122.0	128.7[d] 128.0[d] 127.8[d]	52.7 28.4 27.1 24.7

[a] Measured in [D_6]DMSO at 298 K. [b] Purine numbering. [c] Systematic numbering. [d] Tentative.

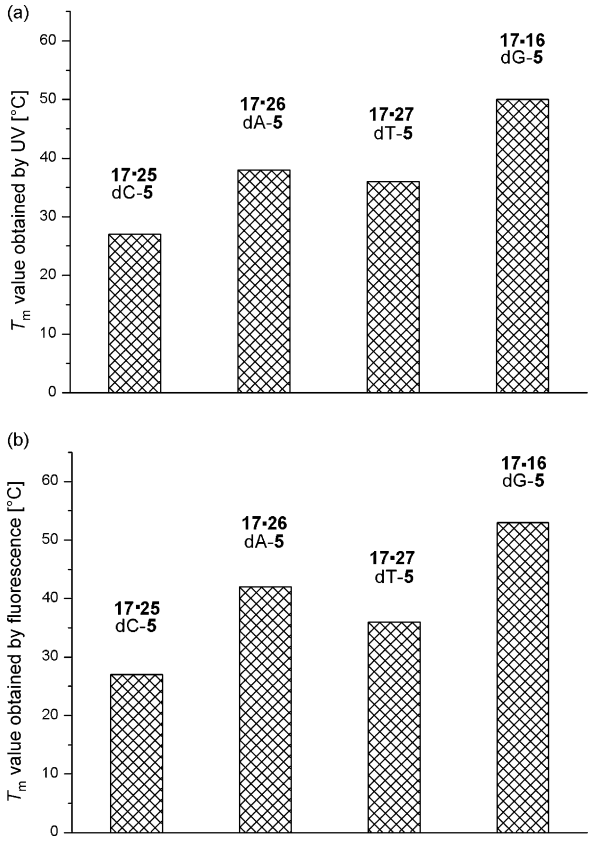

Figure 3. a) Bar diagram reflecting the T_m values obtained from UV melting measured in 0.1 M NaCl, 10 mM $MgCl_2$, 10 mM Na-cacodylate, pH 7.0 with 3+3 μM single strand concentration. b) Bar diagram reflecting the T_m values obtained from fluorescence melting measured in 0.1 M NaCl, 10 mM $MgCl_2$, 10 mM Na-cacodylate, pH 7.0 with 5+5 μM single strand concentration. For original spectra see Figures S13–S16 in the Supporting Information.

and therefore fluorescence is not significantly reduced by nearest-neighbor influences. Only the base pair of **1b** with dG constitutes a noticeable exception[17] as fluorescence is strongly quenched, most probably by hydrogen bonding.[11a]

Our laboratory and others have demonstrated a new concept to elucidate single-nucleotide polymorphism (SNP) by using base-discriminating nucleosides.[5b,27] In this approach, nucleobases can clearly distinguish between matches and mismatches by fluorescence changes. We reasoned that nucleoside **5** meets the above-mentioned requirements and is, therefore, an ideal nucleoside in steady-state fluorescence sensing experiments.

Fluorescence sensing experiments with duplexes containing **5** were carried out at room temperature (22 °C; 0.1 M NaCl or 1 M NaCl) (Figure 4 and Supporting Information). Additionally, the single-stranded (ss) oligonucleotide **17** was measured and duplexes incorporating nucleoside **4** were used for comparison. Surprisingly, the single-stranded oligonucleotide **17** incorporating **5** shows almost the same quantum yield as the free nucleoside **5** ($\Phi = 0.32$ for **5** and $\Phi = 0.29$ for **17**). When nucleoside **5** forms a mismatch with dC in an otherwise complementary duplex, its fluorescence is even higher than in single-stranded DNA (ds **17•25**, Figure 4a,b). In contrast, the perfectly matched oligonucleotide duplex with **5** opposite to dG (**17•16**) shows strong fluorescence quenching (Figure 4a,b). The overall fluorescence intensity decreases according to the following order: dC > dA > dT > dG. The same order is obtained for the low fluorescent compound **4** (Figure 4c,d). However, the discrimination among the various nucleobases is better and more sensitive ($\Phi = 0.32$ for **5** vs. $\Phi = 0.03$ for **4**) for **5** than for **4**. In both cases, the single strands **17** or **21** show lower fluorescence than duplexes forming dC mismatches with **4** or **5**.

As the T_m value of duplex **17•25** with the **5**-dC mismatch is rather low (27 °C), we reasoned that in this case the

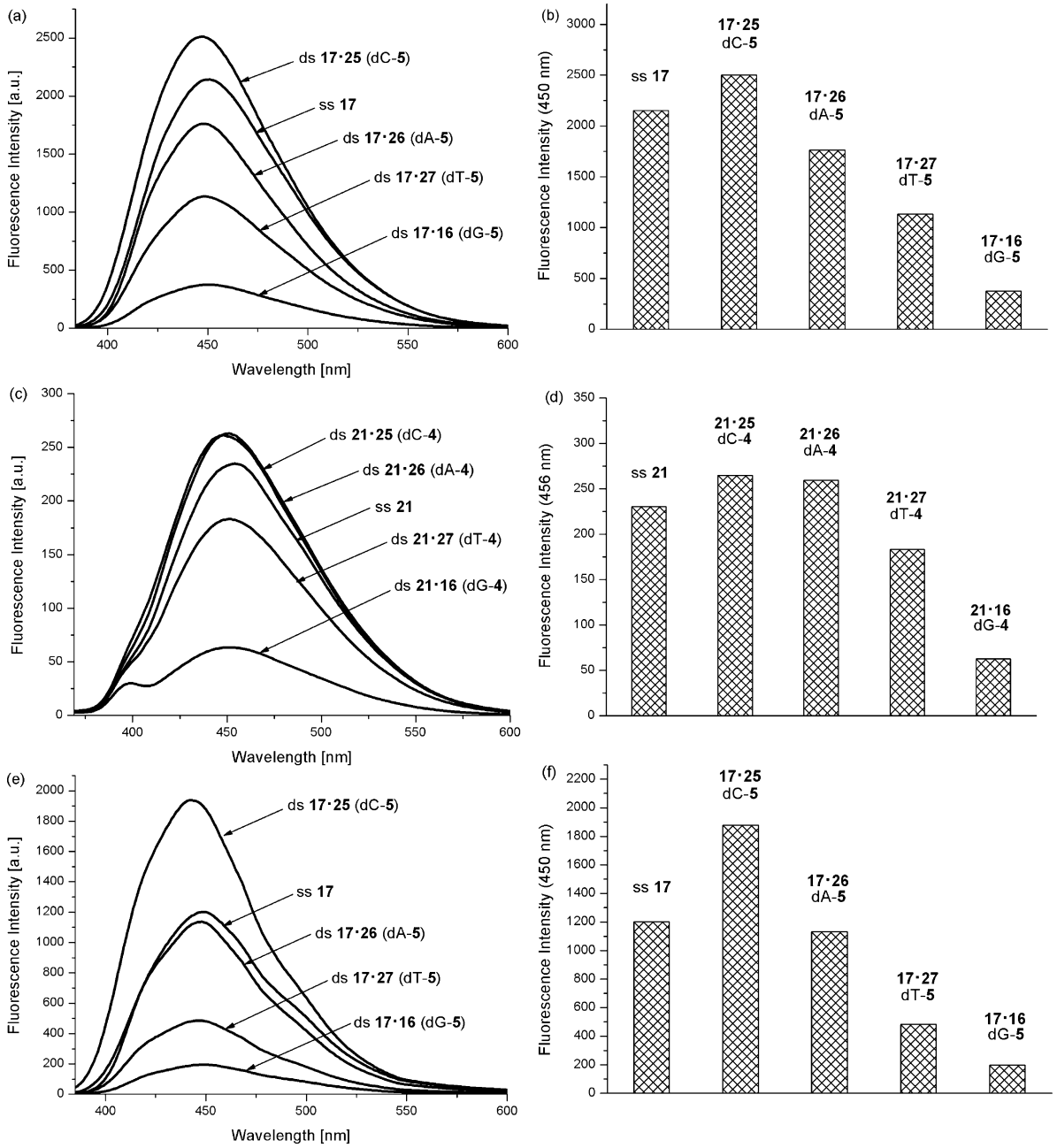

Figure 4. a) Fluorescence spectra of oligonucleotide duplexes **17·25**, **17·26**, **17·27**, and **17·16** containing the benzyl click conjugate **5** and ss oligonucleotide **17** measured at room temperature with 3+3 μM single-strand concentration. b) Bar diagram showing the fluorescence intensities of **5** (data taken from a). c) Fluorescence spectra of oligonucleotide duplexes **21·25**, **21·26**, **21·27** and **21·16** containing the benzyl click conjugate **4** and ss oligonucleotide **21** measured at room temperature with 3+3 μM single-strand concentration. d) Bar diagram showing the fluorescence intensities of **4** (data taken from c). e) Fluorescence spectra of oligonucleotide duplexes **17·25**, **17·26**, **17·27**, **17·16**, and ss oligonucleotide **17** measured at 10°C with 5+ 5 μM single-strand concentration. f) Bar diagram showing the fluorescence intensities of **5** (data taken from e). All measurements were performed in 0.1 M NaCl, 10 mM $MgCl_2$, and 10 mM Na-cacodylate (pH 7.0). For oligonucleotide sequences, see Table 3.

duplex is partially dissociated when fluorescence sensing was performed at 22°C. Therefore, fluorescence sensing was remeasured at 10°C (Figure 4e,f).

In both graphs (10°C and 22°C), the fluorescence intensity of the dC-**5** mismatch (**17·25**) is higher than that of the corresponding single strand ss **17**. Moreover, the fluorescence difference between ss **17** and duplex **17·25** is even more pronounced. This points to the fact that the fully developed duplex was not formed at 22°C but exists at 10°C. According to the T_m melting profiles shown in Figures S13-S14 (Supporting Information) all molecules containing **5** exist as duplexes at 10°C.

To demonstrate that fluorescence sensing with compound **5** is selective for matches or mismatches, we investigated fluorescence changes caused by mismatches positioned far-off the modification site (Figure 5a,b). For these experi-

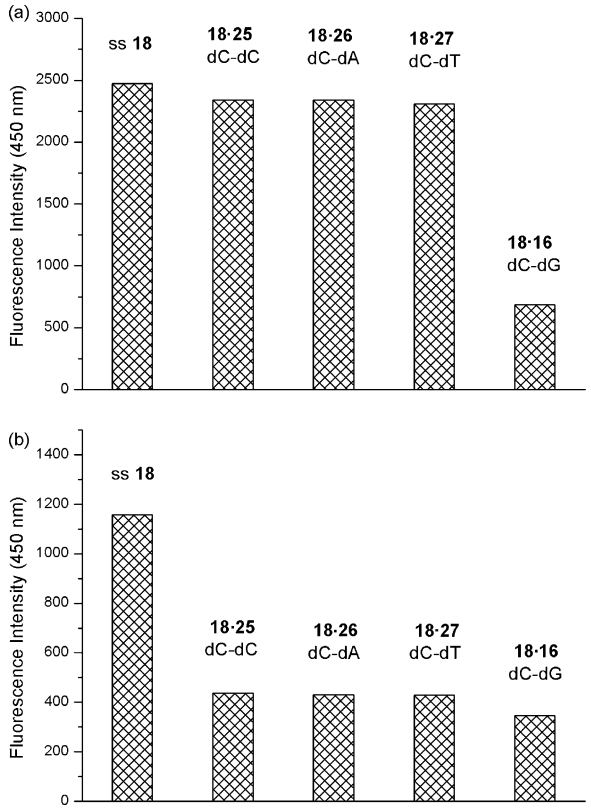

Figure 5. a) Bar diagram showing the fluorescence intensities of oligonucleotide duplexes **18·25**, **18·26**, **18·27**, and **18·16** containing **5** and ss oligonucleotide **18** measured at room temperature with 3+3 μM ss concentration (data taken from Figure S12a in the Supporting Information). b) Bar diagram showing the fluorescence intensities of duplexes **18·25**, **18·26**, **18·27**, and **18·16** containing **5** and ss **18** measured at 10 °C with 5+5 μM ss concentration (data taken from Figure S12b in the Supporting Information).

ments, nucleoside **5** is positioned at the periphery of the duplexes and base pairs always with dG, while a mismatch of a canonical base is situated in the center at a distant site of four base pairs (Table 3, lower section). This is different to the experiments described above, in which the sensor molecules **4** or **5** were always constituents of the matched or mismatched base pair of interest.

Now, the sensor molecule is not able to distinguish among the mismatches far-off the sensor site. Only the transition from duplexes to single strands can be monitored.

Conclusion

New pyrrolo-dC click adducts (**4** and **5**) with 1,2,3-triazole tethers were synthesized, converted into phosphoramidites, and incorporated into oligonucleotides. The fluorescence quantum yield of nucleoside **5** ($\Phi = 0.32$) is about 10 times higher than that of ^{me}pyrrolo-dC (**1b**, $\Phi = 0.026$) or the long linker derivative **4** ($\Phi = 0.03$). Duplexes with single or multiple incorporation of **5** are equally or even more stable than those incorporating canonical dC. Both compounds distinguish between base-pair matches and mismatches when placed opposite to canonical DNA constituents as reflected by T_m changes determined by UV or fluorescence. Compared to the single-stranded oligonucleotide **17**, fluorescence increases in mismatches with **5**-dC, but decreases when **5** is positioned opposite to dA or dT. For nucleoside **5**, base-pair stability determined by fluorescence sensing decreases in the order of dG > dT > dA > dC. The high quantum yield of **5**, its tridentate base pairing ability, and its excellent discriminatory properties make this nucleoside advantageous over conventional nucleoside analogues with intrinsic fluorescence. In addition, nucleobase fluorescence sensing with compound **5** can overcome limitations in SNP detection performed by high-resolution melting (HRM) as the method is not restricted to short DNA fragments.

Experimental Section

6-[1-Benzyl-1*H*-(1,2,3)-triazole-4-yl]-3-(2-deoxy-β-D-*erythro*-pentofuranosyl)furano[2,3-*d*]pyrimidin-2(3*H*)one (7): $CuSO_4$ (15 mg, 0.092 mmol), sodium ascorbate (36 mg, 0.18 mmol), and benzoic acid (5.6 mg, 0.042 mmol) were added to a solution of compound **3a** (115 mg, 0.42 mmol) and benzyl azide (74 μL, 0.59 mmol) in H_2O/*t*BuOH (1:2, 6 mL). The reaction mixture was stirred at RT overnight. The solvent was evaporated and the remaining residue was adsorbed on silica gel and purified by flash chromatography (FC) (silica gel, column 10×3 cm, CH_2Cl_2/CH_3OH 15:1) to afford **7** (120 mg, 70%) as a white solid. R_f = 0.35 (CH_2Cl_2/MeOH 9:1); ^{1}H NMR (300 MHz, [D$_6$]DMSO, 25 °C): δ = 2.09 (m, 1H; 2′-H$_\alpha$), 2.42 (m, 1H; 2′-H$_\beta$), 3.66 (m, 2H; 5′-H), 3.93 (m, 1H; 4′-H), 4.24 (m, 1H; 3′-H), 5.15 (t, ^3J(H,H) = 5.1 Hz, 1H; 5′-OH), 5.31 (d, ^3J(H,H) = 4.2 Hz, 1H; 3′-OH), 5.68 (s, 2H; CH_2), 6.17 (t, ^3J-(H,H) = 6.3 Hz, 1H; 1′-H), 7.08 (s, 1H; 5-H), 7.37 (m, 5H; Ar-H), 8.74 (s, 1H; N=CH), 8.85 ppm (s, 1H; 4-H); UV/Vis (MeOH): λ_{max} (ε) = 343 (13700), 268 nm (22000 mol^{-1} dm^3 cm^{-1}); elemental analysis calcd (%) for $C_{20}H_{19}N_5O_5$: C 58.68, H 4.68, N 17.11; found: C 58.78, H 4.58, N 16.99.

6-[1-Benzyl-1*H*-(1,2,3)-triazole-4-yl]-3-(2-deoxy-β-D-*erythro*-pentofuranosyl)pyrrolo[2,3-*d*]pyrimidin-2(3*H*)one (5): A solution of compound **11** (120 mg, 0.17 mmol) in CH_2Cl_2 (15 mL) was cooled in an ice bath. Then 2.5% dichloroacetic acid (10 mL) was added, the reaction mixture was stirred at 0 °C for 30 min and then neutralized with triethylamine (10 mL). The solvent was removed under vacuum, the remaining residue was adsorbed on silica gel, and purified by FC (silica gel, column 10× 3 cm, CH_2Cl_2/MeOH 9:1) to afford **5** (60 mg, 87%) as a yellow solid. R_f = 0.35 (CH_2Cl_2/MeOH 9:1); ^{1}H NMR (300 MHz, [D$_6$]DMSO, 25 °C): δ = 2.02 (m, 1H; 2′-H$_\alpha$), 2.36 (m, 1H; 2′-H$_\beta$), 3.66 (m, 2H; 5′-H), 3.90 (m, 1H; 4′-H), 4.25 (m, 1H; 3′-H), 5.13 (t, ^3J(H,H) = 5.1 Hz, 1H; 5′-OH), 5.28 (d, ^3J(H,H) = 4.2 Hz, 1H; 3′-OH), 5.69 (s, 2H; CH_2), 6.25 (t, ^3J-(H,H) = 6.3 Hz, 1H; 1′-H), 6.62 (s, 1H; 5-H), 7.39 (m, 5H; Ar-H), 8.45 (s, 1H; N=CH), 8.70 (s, 1H; 4-H), 11.77 ppm (s, 1H; NH); UV/Vis (MeOH): λ_{max} (ε) = 359 (8500), 248 nm (35400 mol^{-1} dm^3 cm^{-1}); elemental analysis calcd (%) for $C_{20}H_{20}N_6O_4$: C 58.82, H 4.94, N 20.58; found: C 58.68, H 5.09, N 20.42.

1-Benzyl-4-ethynyl-1*H*-1,2,3-triazole (9): A mixture of benzyl azide (**6**) (0.73 mL, 5.87 mmol), 1,4-{[bis(trifluoromethyl)]silyl}buta-1,3-diyne (**8**) (2.02 g, 8.20 mmol), CuBr (126 mg, 0.88 mmol), Et_3N (1.6 mL, 11.74 mmol), and H_2O (0.2 mL, 11.74 mmol) in DMF (5 mL) was heated at 100 °C for 3.5 h. The reaction was diluted with CH_2Cl_2 (50 mL) and washed with H_2O (2×50 mL). The organic layer was dried over Na_2SO_4, filtered, and evaporated to dryness. The residue was purified by FC (silica gel, column 10×3 cm, PE/EtOAc 5:1) to afford **9** as a white solid (538 mg, 50%). R_f = 0.35 (PE/EtOAc 3:2); ^{1}H NMR (300 MHz, [D$_6$]DMSO, 25 °C): δ = 4.42 (s, 1H; C≡CH), 5.61 (s, 2H; CH_2), 7.36 (m,

5H; Ar-H), 8.56 ppm (s, 1H; N=CH); elemental analysis calcd (%) for $C_{11}H_9N_3O$: C 72.11, H 4.95, N 22.94; found: C 71.99, H 5.05, N 22.69.

6-[1-Benzyl-1*H*-(1,2,3)-triazole-4-yl]-3-[2-deoxy-5-*O*-(4,4′-dimethoxytriphenylmethyl)-*β*-D-*erythro*-pentofuranosyl]pyrrolo[2,3-*d*]pyrimidin-2(3*H*)one (11): A mixture of **9** (366.4 mg, 2.0 mmol), **10** (759.6 mg, 1.0 mmol), $[PdCl_2(PPh_3)_2]$ (70.2 mg, 0.1 mmol), and CuI (38 mg, 0.2 mmol) in Et_3N (6 mL) and DMF (8 mL) was heated at 50 °C for 24 h. The reaction mixture was diluted with CH_2Cl_2 (50 mL) and washed with H_2O (2×20 mL). The organic phase was dried over Na_2SO_4, filtered, and evaporated to dryness. The residue was purified by FC (silica gel, column 10×3 cm, CH_2Cl_2/CH_3OH 30:1) to afford **11** (355 mg, 50%) as a yellow foam. R_f=0.30 (CH_2Cl_2/MeOH 9:1); ^{1}H NMR (300 MHz, [D$_6$]DMSO, 25 °C): δ=2.18 (m, 1H; 2′-H$_\alpha$), 2.42 (m, 1H; 2′-H$_\beta$), 3.29 (m, 2H; 5′-H), 3.69 (s, 3H; OCH_3), 3.70 (s, 3H; OCH_3), 4.01 (m, 1H; 4′-H), 4.39 (m, 1H; 3′-H), 5.40 (d, ^3J(H,H)=4.8 Hz, 1H; 3′-OH), 5.69 (s, 2H; CH_2), 5.98 (s, 1H; 5-H), 6.25 (t, ^3J(H,H)=5.4 Hz, 1H; 1′-H), 7.15 (m, 18H; Ar-H), 8.39 (s, 1H; N=CH), 8.60 (s, 1H; 4-H), 11.77 ppm (s, 1H; NH); UV/Vis (MeOH): λ_{max} (ε)=359 (9100), 238 nm (44000 mol^{-1} dm^3 cm^{-1}); elemental analysis calcd (%) for $C_{41}H_{38}N_6O_6$: C 69.28, H 5.39, N 11.82; found: C 69.10, H 5.16, N 11.71.

6-[1-Benzyl-1*H*-(1,2,3)-triazole-4-yl]-3-[2-deoxy-5-*O*-(4,4′-dimethoxytriphenylmethyl)-*β*-D-*erythro*-pentofuranosyl]pyrrolo[2,3-*d*]pyrimidin-2(3*H*)one 3′-[(2-cyanoethyl)-(*N*,*N*-diisopropyl)]phosphoramidite (12): (iPr)$_2$EtN (70 μL, 0.41 mmol) and 2-cyanoethyl *N*,*N*-diisopropylphosphoramido chloridite (65 μL, 0.29 mmol) were added to a solution of **11** (147 mg, 0.21 mmol) in dry CH_2Cl_2 (8 mL). The solution was stirred at RT for 30 min. The solution was diluted with CH_2Cl_2 (40 mL) and washed with a 5% aq. $NaHCO_3$ solution. The mixture was extracted with CH_2Cl_2 (2×20 mL). The combined organic phase was dried (Na_2SO_4), filtered, and evaporated. The residue was purified by FC (silica gel, column 15×5 cm, CH_2Cl_2/MeOH 30:1) to afford crude **12** as a yellow foam. The foamy residue was dissolved in CH_2Cl_2 (2 mL) and added gradually to stirring cyclohexane (50 mL) cooled to −30 °C. The precipitate was isolated by filtration and the resulting powder was dried under vacuum, yielding **12** (142 mg, 75%) as a yellow foam. R_f=0.44 (CH_2Cl_2/MeOH 20:1); ^{31}P NMR (121.5 MHz, $CDCl_3$, 25 °C): δ=149.30, 148.70 ppm.

6-{4-[1-Benzyl-1*H*-(1,2,3)-triazole-4-yl]butyl}-3-(2-deoxy-*β*-D-*erythro*-pentofuranosyl)pyrrolo[2,3-*d*]pyrimidin-2(3*H*)one (4): Benzyl azide (**6**) (262 μL, 2.09 mmol) was added to a mixture of **2b** (532 mg, 1.61 mmol), $CuSO_4$ (51 mg, 0.32 mmol), sodium ascorbate (128 mg, 0.64 mmol), and benzoic acid (20 mg, 0.16 mmol) in H_2O/*t*BuOH (2:1, 9 mL). The reaction mixture was stirred for 24 h at RT. The solvent was evaporated and the remaining residue was adsorbed on silica gel and purified by FC (silica gel, column 10×3 cm, CH_2Cl_2/MeOH 9:1) to afford **4** as a white solid (658 mg, 88%). R_f=0.35 (CH_2Cl_2/MeOH 4:1); ^{1}H NMR (300 MHz, [D$_6$]DMSO, 25 °C): δ=1.62 (m, 4H; 2×CH_2), 1.99 (m, 1H; 2′-H$_\alpha$), 2.32 (m, 1H; 2′-H$_\beta$), 2.55 (m, 2H; CH_2), 2.62 (m, 2H; CH_2), 3.55 (m, 2H; 5′-H), 3.87 (m, 1H; 4′-H), 4.23 (m, 1H; 3′-H), 5.11 (s, 1H; 5′-OH), 5.26 (s, 1H; 3′-OH), 5.52 (s, 2H; CH_2), 5.89 (s, 1H; 5-H), 6.26 (t, ^3J(H;H)=6.3 Hz, 1H; 1′-H), 7.33 (m, 5H; Ar-H), 7.89 (s, 1H; N=CH), 8.50 (s, 1H; 4-H), 11.13 ppm (s, 1H; NH); UV/Vis (MeOH): λ_{max} (ε)=343 (4300), 263 (4100), 218 nm (32800 mol^{-1} dm^3 cm^{-1}); elemental analysis calcd (%) for $C_{24}H_{28}N_6O_4$: C 62.06, H 6.08, N 18.09; found: C 61.91, H 6.10, N 17.98.

6-{4-[1-Benzyl-1*H*-(1,2,3)-triazole-4-yl]butyl}-3-[2-deoxy-5-*O*-(4,4′-dimethoxytriphenylmethyl)-*β*-D-*erythro*-pentofuranosyl]pyrrolo[2,3-*d*]pyrimidin-2(3*H*)one (13): Compound **4** (639 mg, 1.38 mmol) was dried by co-evaporation with dry pyridine (3×10 mL) and then dissolved in dry pyridine (20 mL). DMT-chloride (606 mg, 1.79 mmol) was added in three portions in 4 h and the reaction mixture was stirred overnight. MeOH (2 mL) was added and stirring was continued for 5 min. Then, the solvent was removed and the remaining residue was dissolved in CH_2Cl_2 (50 mL) and washed with a 5% aq. $NaHCO_3$ solution (20 mL). The organic layer was dried over Na_2SO_4, filtered, and evaporated to dryness. The residue was purified by FC (CH_2Cl_2/CH_3OH 25:1) to afford **13** as a white solid (720 mg, 68%). R_f=0.56 (CH_2Cl_2/MeOH 9:1); ^{1}H NMR (300 MHz, [D$_6$]DMSO, 25 °C): δ=1.59 (m, 4H; 2×CH_2), 2.14 (m, 1H; 2′-H$_\alpha$), 2.38 (m, 1H; 2′-H$_\beta$), 2.56 (m, 2H; 2x CH_2), 3.29 (m, 2H; 5′-H), 3.71 (s, 6H; 2×OCH_3), 3.97 (m, 1H; 4′-H), 4.38 (m, 1H; 3′-H), 5.22 (s, 1H; 5-H), 5.39 (d, ^3J(H,H)=4.5 Hz, 1H; 3′-OH), 5.52 (s, 2H; CH_2), 6.25 (t, ^3J(H,H)=5.7 Hz, 1H; 1′-H), 7.14 (m, 18H; Ar-H), 7.88 (s, 1H; N=CH), 8.40 (s, 1H; 4-H), 11.11 ppm (s, 1H; NH); UV/Vis (MeOH): λ_{max} (ε)=343 (4300), 231 nm (47000 mol^{-1} dm^3 cm^{-1}); elemental analysis calcd (%) for $C_{45}H_{46}N_6O_6$: C 70.48, H 6.05, N 10.96; found: C 70.49, H 6.08, N 10.85.

6-{4-[1-Benzyl-1*H*-(1,2,3)-triazole-4-yl]butyl}-3-[2-deoxy-5-*O*-(4,4′-dimethoxytriphenylmethyl)-*β*-D-*erythro*-pentofuranosyl]pyrrolo[2,3-*d*]pyrimidin-2(3*H*)one 3′-[(2-cyanoethyl)-(*N*,*N*-diisopropyl)]phosphoramidite (14): (iPr)$_2$EtN (146 μL, 0.86 mmol) and 2-cyanoethyl *N*,*N*-diisopropylphosphoramido chloridite (0.157 μL, 0.70 mmol) were added to a solution of **13** (412 mg, 0.54 mmol) in dry CH_2Cl_2 (10 mL). The solution was stirred at RT for 15 min. The solution was diluted with CH_2Cl_2 (40 mL) and washed with a 5% aq. $NaHCO_3$ solution. The aq. phase was extracted with CH_2Cl_2 (2×20 mL) and the combined organic phase was dried (Na_2SO_4), filtered, and evaporated. The residue was purified by FC (silica gel, column 15×5 cm, CH_2Cl_2/MeOH 40:1) to afford **14** as a white foam. The foamy residue was dissolved in CH_2Cl_2 (3 mL) and added gradually to a vigorously stirred solution of pre-cooled (−30 °C) cyclohexane (80 mL). A precipitate was formed that was isolated by filtration. The resulting powder was dried under vacuum, yielding **14** as a colorless foam (290 mg, 56%). R_f=0.44 (CH_2Cl_2/MeOH 20:1); ^{31}P NMR (121.5 MHz, $CDCl_3$, 25 °C): δ=149.30, 148.70 ppm.

Acknowledgements

We thank Mr. H. Mei for carrying out the fluorescence melting studies. We thank Mr. S.S. Pujari for the measurement of the NMR spectra and Mr. N.Q. Tran for the oligonucleotide synthesis. We are grateful to Dr. P. Leonard and Dr. S. Budow for their continuous support throughout the preparation of the manuscript. Financial support from ChemBiotech, Münster, Germany is gratefully acknowledged.

[1] a) J. R. Lakowicz, *Principles of Fluorescence Spectroscopy*, Springer, New York, **2006**; b) H.-A. Wagenknecht, *Charge Transfer in DNA: From Mechanism to Application*, Wiley-VCH, Weinheim, **2005**.
[2] a) R. W. Sinkeldam, N. J. Greco, Y. Tor, *Chem. Rev.* **2010**, *110*, 2579–2619; b) M. S. T. Gonçalves, *Chem. Rev.* **2009**, *109*, 190–212.
[3] L. M. Wilhelmsson, *Q. Rev. Biophys.* **2010**, *43*, 159–183.
[4] a) J. Gao, H. Liu, E. T. Kool, *J. Am. Chem. Soc.* **2004**, *126*, 11826–11831; b) H. Lu, K. He, E. T. Kool, *Angew. Chem.* **2004**, *116*, 5958–5960; *Angew. Chem. Int. Ed.* **2004**, *43*, 5834–5836.
[5] a) D. W. Dodd, R. H. E. Hudson, *Mini-Rev. Org. Chem.* **2009**, *6*, 378–391; b) A. Okamoto, Y. Saito, I. Saito, *J. Photochem. Photobiol. C* **2005**, *6*, 108–122.
[6] H. Inoue, A. Imura, E. Ohtsuka, *Nippon Kagaku Kaishi* **1987**, *7*, 1214–1220.
[7] a) F. Seela, E. Schweinberger, K. Xu, V. R. Sirivolu, H. Rosemeyer, E.-M. Becker, *Tetrahedron* **2007**, *63*, 3471–3482; b) Y.-H. Koh, J. H. Shim, J.-L. Girardet, Z. Hong, *Bioorg. Med. Chem. Lett.* **2007**, *17*, 5261–5264.
[8] F. Seela, X. Peng, S. Budow, *Curr. Org. Chem.* **2007**, *11*, 427–462.
[9] F. Seela, Y. Chen, *Nucleic Acids Res.* **1995**, *23*, 2499–2505.
[10] D. A. Berry, K.-Y. Jung, D. S. Wise, A. D. Sercel, W. H. Pearson, H. Mackie, J. B. Randolph, R. L. Somers, *Tetrahedron Lett.* **2004**, *45*, 2457–2461.
[11] a) C. Liu, C. T. Martin, *J. Mol. Biol.* **2001**, *308*, 465–475; b) C. Liu, C. T. Martin, *J. Biol. Chem.* **2002**, *277*, 2725–2731.
[12] P. Chen, C. He, *J. Am. Chem. Soc.* **2004**, *126*, 728–729.
[13] N. P. Johnson, W. A. Baase, P. H. von Hippel, *Proc. Natl. Acad. Sci. USA* **2005**, *102*, 7169–7173.
[14] C. Dash, J. W. Rausch, S. F. J. Le Grice, *Nucleic Acids Res.* **2004**, *32*, 1539–1547.
[15] F. Seela, V. R. Sirivolu, *Org. Biomol. Chem.* **2008**, *6*, 1674–1687.
[16] a) P. M. E. Gramlich, C. T. Wirges, A. Manetto, T. Carell, *Angew. Chem.* **2008**, *120*, 8478–8487; *Angew. Chem. Int. Ed.* **2008**, *47*, 8350–

8358; b) H. C. Kolb, M. G. Finn, K. B. Sharpless, *Angew. Chem.* **2001**, *113*, 2056–2075; *Angew. Chem. Int. Ed.* **2001**, *40*, 2004–2021; c) A. H. El-Sagheer, T. Brown, *Chem. Soc. Rev.* **2010**, *39*, 1388–1405.
[17] S. J. O. Hardman, S. W. Botchway, K. C. Thompson, *Photochem. Photobiol.* **2008**, *84*, 1473–1479.
[18] a) A. Dierckx, P. Dinér, A. H. El-Sagheer, J. D. Kumar, T. Brown, M. Grøtli, L. M. Wilhelmsson, *Nucleic Acids Res.* **2011**, *39*, 4513–4524; b) C. Dyrager, K. Börjesson, P. Dinér, A. Elf, B. Albinsson, L. M. Wilhelmsson, M. Grøtli, *Eur. J. Org. Chem.* **2009**, 1515–1521.
[19] a) A. P. Demchenko, *Trends Biotechnol.* **2005**, *23*, 456–460; b) E. A. Lemke, C. Schultz, *Nat. Chem. Biol.* **2011**, *7*, 480–483.
[20] a) N. J. Greco, Y. Tor, *Tetrahedron* **2007**, *63*, 3515–3527; b) R. H. E. Hudson, A. Ghorbani-Choghamarani, *Synlett* **2007**, 0870–0873; c) M. A. Ivanov, A. V. Ivanov, I. A. Krasnitskaya, O. A. Smirnova, I. L. Karpenko, E. F. Belanov, V. S. Prasolov, V. L. Tunitskaya, L. A. Alexandrova, *Russ. J. Bioorg. Chem.* **2008**, *34*, 593–601.
[21] M. J. Robins, K. Miranda, V. K. Rajwanshi, M. A. Peterson, G. Andrei, R. Snoeck, E. De Clercq, J. Balzarini, *J. Med. Chem.* **2006**, *49*, 391–398.
[22] a) F. Wojciechowski, R. H. E. Hudson, *J. Am. Chem. Soc.* **2008**, *130*, 12574–12575; b) S. R. Gerrard, M. M. Edrees, I. Bouamaied, K. R. Fox, T. Brown, *Org. Biomol. Chem.* **2010**, *8*, 5087–5096; c) F. Wojciechowski, R. H. E. Hudson, *Org. Lett.* **2009**, *11*, 4878–4881.
[23] F. Cuevas, A. I. Oliva, M. A. Pericàs, *Synlett* **2010**, 1873–1877.
[24] A. S. Wahba, A. Esmaeili, M. J. Damha, R. H. E. Hudson, *Nucleic Acids Res.* **2010**, *38*, 1048–1056.
[25] P. J. Bates, C. A. Laughton, T. C. Jenkins, D. C. Capaldi, P. D. Roselt, C. B. Reese, S. Neidle, *Nucleic Acids Res.* **1996**, *24*, 4176–4184.
[26] a) C. Dohno, I. Saito, *ChemBioChem* **2005**, *6*, 1075–1081; b) A. Okamoto, K. Tanaka, T. Fukuta, I. Saito, *J. Am. Chem. Soc.* **2003**, *125*, 9296–9297; c) A. Okamoto, K. Tainaka, I. Saito, *J. Am. Chem. Soc.* **2003**, *125*, 4972–4973.
[27] a) D. Jiang, F. Seela, *J. Am. Chem. Soc.* **2010**, *132*, 4016–4024; b) F. Seela, D. Jiang, K. Xu, *Org. Biomol. Chem.* **2009**, *7*, 3463–3473.
[28] V. Zozulya, A. Shcherbakova, I. Dubey, *J. Fluoresc.* **2000**, *10*, 49–53.
[29] M. J. Rist, J. P. Marino, *Curr. Org. Chem.* **2002**, *6*, 775–793.
[30] F. Seela, G. Becher, *Helv. Chim. Acta* **2000**, *83*, 928–942.

Received: October 27, 2011
Revised: April 17, 2012
Published online: July 5, 2012

